DO HIGH FREQUENCY ACOUSTIC EMISSION EVENTS ALWAYS REPRESENT FIBRE FAILURE IN CFRP LAMINATES?

Fatih E. Oz, Nuri Ersoy and Stepan V. Lomov

DO HIGH FREQUENCY ACOUSTIC EMISSION EVENTS ALWAYS REPRESENT FIBRE FAILURE IN CFRP LAMINATES?

Fatih E. Oz[1], Nuri Ersoy[1] and Stepan V. Lomov[2]

[1]Department of Mechanical Engineering, Bogazici University, Bebek, 34342, Istanbul, Turkey
Email: fatih.oz@boun.edu.tr, nuri.ersoy@boun.edu.tr
[2]Department of Materials Engineering, KU Leuven, Kasteelpark Arenberg 44, 3001 Leuven, Belgium
Email: stepan.lomov@kuleuven.be

ABSTRACT. When damage in carbon fibre reinforced composites (CFRP) is monitored by acoustic emission (AE), it is a common belief that high frequency AE events originate from fibre failure. Tihs shows that this statement may not correspond to the reality, and matrix cracks can emit high frequency AE signals. Quasi-static tension of $[-45_2/0_2/+45_2/90_2]_s$ laminates was monitored by AE, Digital Image Correlation (DIC) on the surface of the sample and in-situ optical microscopy on the sample's polished edge. Unsupervised k-means clustering algorithm was applied to the AE results. By comparison with the direct DIC and microscopic observations, the AE cluster with high frequency and low amplitude was found to correspond to directly observed matrix cracks.

Keywords: Polymer-matrix composites (PMCs), Acoustic emission, Transverse cracking, Delamination

1. INTRODUCTION

Acoustic Emission (AE) registration allows monitoring damage during mechanical loading of composite materials. Cluster analysis of the multi-parametrical AE signals is a commonly used method for their classification and identification of the damage mode which caused an AE event [1–4]; the spatial position of the signal source can be identified when two AE sensors are used. Peak frequency and the signal amplitude are assumed to be the most important AE parameters for damage classification. There is a common conclusion in literature that AE signals with high peak frequency correspond to fibre failure [2–10]. This conclusion is relied on different reasons, such as; optical observations after final failure [3,7,9], fibre failure predictions with numerical or analytical methods [4,10], models of AE propagation [3] and results from single constituents' tests [5,8,10–12]. The

identification of the high frequency events is often non-critically used as an established fact [4,13,14]. However, a strong, actual, “in-situ” evidence to prove this interpretation has not been presented yet. Moreover, there exist observations which point to the contrary. Baker et. al. [15], and Maillet et. al. [16] have shown that matrix cracking in cross-ply laminates can also generate high frequency AE events due to transverse matrix cracks in 90° plies and that an identification of the damage mode requires more detailed analysis of the acoustic wave propagation and attenuation in the laminate.

In the present paper we report results of simultaneous monitoring of damage in quasi-isotropic (QI) $[-45_2/0_2/+45_2/90_2]_s$ laminates under quasi-static tension with AE, Digital Image Correlation (DIC) on the sample surface and microscopic crack observation on the sample’s edge, which shows by direct optical observations that matrix cracking in the 90° and ±45° layers generate AE events with weighted frequency over 260 kHz and amplitude below 66 dB, which a number of studies [2,3,5–12] classify as fibre failure. We want to draw the reader’s attention to the title question “Do high frequency acoustic emission events always represent fibre failure in CFRP laminates?”, to which our results, based on the direct observation of the damage in correlation with AE registration, give a negative answer.

2. MATERIAL AND EXPERIMENTAL METHODOLOGY

Material used in this study is Hexcel’s AS4/8552. Its fibre volume fraction and nominal thickness are 57.4 % and 0.184 mm respectively. QI plates were manufactured according to the Manufacturer’s Recommended Cure Cycle (MRCC) in an autoclave at Boğaziçi University’s Composites Laboratory. Specimens were cut with a diamond saw and prepared according to ASTM 3039 Standard [17]. $[-45_2/0_2/+45_2/90_2]_s$ specimens with 3 mm thickness, 15 mm width and 175 mm length are tested in this study. QI GFRP composites with 1.5 mm thickness and 50 mm length are used for

end tabs. Their gage section ends are tapered to 20°-30° to minimize stress concentrations and prevent failure from grip sections.

Multi-instrument in-situ monitoring techniques are applied in this study. The tests are performed with electro-mechanical Instron 4505 universal testing machine with a rate of 1 mm/min. Real time AE monitoring with Vallen AMSY-5 system is applied with two broadband Digital Wave B-1025 AE sensors (frequency range 25-1600 kHz). Distance between the sensors is 50 mm. The AE events location was determined by standard AMSY algorithms based on the difference in the signals arrival times. Using only AE registration technique during tension tests is not sufficient to identify damage modes and correlate them with corresponding AE events. So, in addition to AE; DIC is used to observe damage on the sample surface and macro damage in the laminate. One surface of the specimens are speckled for the DIC calculations. Crack observation from a 5 mm region on the sample's edge with a high magnification, high-speed Charge-Coupled Device (CCD) camera shows direct detection of micro damages at inner layers. One edge of the specimen is polished for a clear observation.

Unsupervised k-means++ clustering algorithm, developed by Li et. al. [4] is used to classify the AE events. Details of this algorithm are not given here for the sake of brevity, readers should refer to the cited reference.

3. RESULTS AND DISCUSSION

Results of five tests are reported here. Specimens are loaded up to 70%-80% and 90% of the ultimate strength (540 MPa). In order to show the consistency and repeatability of the tests, stress vs. strain graphs are plotted with two most important AE parameters in Figure 1; note that the end of the stress-strain diagrams corresponds to the test stop and not to the specimen failure. Tests #3 and #5 are performed with all damage monitoring instruments listed before; AE registration to emit stress waves of damage modes, DIC for surface cracks and edge microscopy for micro damage modes at

inner plies. These samples are loaded up to 90% of its ultimate strength. Only AE and DIC are used during quasi-static tension for the rest of the specimens. Figure 1.a shows that test results are highly repeatable. Peak frequency distributions are plotted in Figure 1.b. The pattern of the event frequency is remarkable: it shows high peak frequency values (250…800 kHz) during mid-strain levels and their disappearance afterwards. According to the peak frequency trends cited in literature [2–10] these high peak frequency signals should be due to fibre breakages. However, they are recorded between strain levels of 0.0048-0.0072 (which corresponds to stress levels of 240-320 MPa). So, do fibre breaks start really so early for this laminate, if the failure strain for the AS4 fibres is, according to the data sheet, 0.0182? This question was asked previously by Li et. al [4]. They tried to show a correlation between high frequency AE events with fibre breaks by using a fibre bundle model based on Weibull estimation. Number of high frequency AE events throughout the tests are compared with estimated number of fibre breaks. It showed earlier start of individual fibre breaks than AE cluster for woven fabric yarns. Two reasons were proposed for such discrepancy. Firstly, it was believed that isolated fibre breaks could not create a noticeable AE event and high frequency signals were not recorded during early strain levels. Secondly, Weibull estimates high number of breaks than reality. DIC and edge observations in this study provide an answer to abovementioned question and that is "NO". These high peak frequency events are due to matrix cracks at the inner 90° and 45° plies.

Micro damage and DIC strain maps recorded during test #3 are presented in Figure 2. Test #5 gave the similar results. Coloured regions in Figure 2 are area of interest for DIC calculations. This area is divided into subsets and individual strains are calculated. They consist overall strain maps and shown with colour scales as shown in Figure 2. Average strain values of this area of interest are used for Figure 2. Test direction, $+\varepsilon_1$, and contraction in transverse direction, $\pm\varepsilon_2$, are mentioned on Figure 2. Following Figure 2, the damage sequence is as follows. First damage initiates in 90° plies. It propagates through the adjacent 45° plies. Transverse cracks in the middle 90° and the adjacent 45° plies become visible from the edge at 0.0058 strain level; the same damage pattern is seen at 0.0067

strain. Micro delaminations between 90/45 intersections are also seen, coinciding with transverse cracks. After the strain level of 0.0067, the ε_2 strain map shows separation of the map in two zones. The zone with the "normal" transverse strain values (upper part of the map), corresponding to the low values expected from the low Poisson contraction of the laminate, containing 90° plies, and high negative values (lower part of the map), which evidence much more pronounced Poisson effect. This phenomenon can be attributed to macro delamination, initiated from the unpolished (lower) edge of the specimen. The delaminated plies are not connected to the 90° plies and are free to contract transversely. Appearance of the macro delamination at the end of the test is shown at the bottom of Figure 2. From 0.0067 strain level until the end of the test, macro delaminations on the unpolished edge and the existing micro delaminations between the 90/45 intersections continue to propagate with appearance of new micro delaminations on the polished edge.

This understanding of the sequence of damage is corroborated by different means of optical monitoring used during the test. In-situ edge observations detect micro damage in the 90° and 45° plies, micro delaminations between the 45/90 and the 0/45 plies whereas 2D DIC emphasizes the onset and propagation of the macro delamination. Now we can analyse correspondence of the AE activity and the damage progression.

All the AE events shown in Figure 1 are classified using the clustering algorithm [4]. These clusters are used to correlate the AE events with the observed damage modes. Optimal cluster number is found to be four for all the five tests. Weighted Frequency (WF) and Amplitude (A) are seen to be the most selective parameters for AE clustering. WF is not a directly obtained AE parameter. It is square root of Frequency Centroid and Peak Frequency multiplication. Accumulation of these clusters with respect to WF through tests and summary of cluster groups are shown in Figure 3. According to the cluster groups in Figure 3, 66 dB and 260 kHz are the boundaries which roughly separate the clusters in the amplitude and the frequency scale.

Figure 3 shows the consistency of cluster distributions through each test. It is seen that early damage stage (up to 0.0065 strain) corresponds to high frequency-low amplitude clusters (CL3-CL4). After this strain, CL3-CL4 disappear and low frequency-high amplitude cluster (CL1) starts intensively. At the same time, density of low frequency-low amplitude cluster (CL2) starts to increase.

A correlation between the optical observations (Figure 2) and AE parameters (Figure 3) can be seen for test #3 (Figure 3.c). The only observable damage modes below 0.0067 strain are transverse cracks at inner 90° and 45° plies and micro delaminations between the 90/45 plies in Figure 2. It seems from Figure 3.c that events with high frequencies (CL3-CL4) correspond to this damage mode. In order to support this interpretation, the AE events are filtered to correspond only to the locations imaged in the edge microscopy observations. The edge observation's field of view, shown in Figure 2, corresponds to the distance to the centre of the AE sensor in the range 20 … 25 mm and the distance between the two transverse cracks are 2.4 mm. So, distances of these cracks to location detecting sensor are around 21 mm and 23.5 mm, respectively. Figure 4 shows the location of AE events clusters. The distance of events in CL3-CL4 within the field of view of the edge observation is consistent with optical observations as highlighted in Figure 4, within a position error of about 1 mm. Thus, optical observations and AE location detection justifies the interpretation for correlation of high frequency-low amplitude AE clusters with transverse cracks at the inner 90° and 45° plies.

Cluster CL1 starts intensively at 0.0067 strain in Figure 3.c that is the same strain level with macro delamination seen from the DIC strain map in Figure 2. CL1 is low frequency-high amplitude AE cluster and corresponds to macro delamination which initiates near the unpolished edge.

Cluster CL2 is the AE cluster with the low frequency-low amplitude values. Figure 3.c shows that it is started from early strain levels of the test and its density increases after 0.0067 strain level until the end of the test. Accumulation of this cluster through the tests correspond to micro delaminations occurred between the +45°/90° and +45°/0° intersections. Until 0.0067 strain level, only micro delaminations between the +45°/90° is seen, then after 0.0067 strain level, delaminations between

the +45°/0° boundary can be visible from edge observation as highlighted in Figure 2. The increasing number of these micro delaminations at different plies boundaries correspond to CL2 which has the low frequency-low amplitude properties. The events in this cluster are distributed evenly over the location, as seen in Figure 4.b. Since delaminations involving the 45° plies propagate with this angle through the width of the specimen, this large distribution in Figure 4.b is an expected result and consistent with the interpreted damage mode for CL2.

To summarise, we have identified high frequency events with the matrix cracking in 90° and 45° plies of a QI laminate, in the dynamics of the crack system development. This augments the results of Baker et. al. [15] and Maillet et. al. [16], who previously observed that even though high frequency events can be recorded, the only observed damage was transverse cracks in cross-ply laminates at the end of the tests. Our simultaneous optical damage observations show that high peak frequency events correspond to damage at inner the 90° and 45° plies.

4. CONCLUSION

This paper demonstrates the effectiveness of multi-parameter evaluation for the analysis of AE events. However, it is not sufficient for robust damage mode classification. Application of simultaneous optical observation of the damage on micro-scale and DIC analysis of the strain fields with the experimental results presented in this paper prove that matrix cracks in CFRP laminates can initiate high-frequency AE signals. Therefore, the identification of high-frequency AE events as related to the fibre breakage, often stated in the literature, should be taken with caution.

Our measurements, specifically the correlations between the AE signals parameters and direct optical observation of the damage events, suggest the following classification of the origin of AE events in the studied material: (1) low frequency, low amplitude: microcracking (micro delamination, fibre debonding); (2) low frequency, high amplitude: delaminations; (3) high frequency: matrix transverse

or shear cracks. Whether this correspondence has more general applicability, should be the subject of future work.

We also have observed that 2D DIC measurement can successfully detect macro delaminations at inner plies and that is correlated with high amplitude AE events, registered from the inner plies. The identification of fibre damage by the AE registration on the macro-level is an open question.

ACKNOWLEDGEMENT

Authors acknowledge the support of the Boğaziçi University Research Fund, Istanbul Development Agency (ISTKA) and TUBITAK BIDEB 2214-A under project codes 10020/15A06D3, ISTKA/BIL/2012/58 and 1059B141600673 respectively. S.V. Lomov holds the Toray Chair on Composites at KU Leuven, the support of which is gratefully acknowledged.

REFERENCES

[1] Godin N, Huguet S, Gaertner R, Salmon L. Clustering of acoustic emission signals collected during tensile tests on unidirectional glass/polyester composite using supervised and unsupervised classifiers. {NDT} E Int 2004;37:253–64. doi:https://doi.org/10.1016/j.ndteint.2003.09.010.

[2] Gutkin R, Green CJ, Vangrattanachai S, Pinho ST, Robinson P, Curtis PT. On acoustic emission for failure investigation in CFRP: Pattern recognition and peak frequency analyses. Mech Syst Signal Process 2011;25:1393–407. doi:10.1016/j.ymssp.2010.11.014.

[3] Sause MGR, Müller T, Horoschenkoff A, Horn S. Quantification of failure mechanisms in mode-I loading of fiber reinforced plastics utilizing acoustic emission analysis. Compos Sci Technol 2012;72:167–74. doi:10.1016/j.compscitech.2011.10.013.

[4] Li L, Swolfs Y, Straumit I, Yan X, Lomov S V. Cluster analysis of acoustic emission signals for 2D and 3D woven carbon fiber/epoxy composites. J Compos Mater 2016;50:1921–35. doi:10.1177/0021998315597742.

[5] de Groot PJ, Wijnen PAM, Janssen RBF. Real-time frequency determination of acoustic emission for different fracture mechanisms in carbon/epoxy composites. Compos Sci Technol 1995;55:405–12. doi:10.1016/0266-3538(95)00121-2.

[6] Bohse J. Acoustic emission characteristics of micro-failure processes in polymer blends and composites. Compos Sci Technol 2000;60:1213–26. doi:10.1016/S0266-3538(00)00060-9.

[7] Ramirez-Jimenez CR, Papadakis N, Reynolds N, Gan TH, Purnell P, Pharaoh M. Identification of failure modes in glass/polypropylene composites by means of the primary frequency content of the acoustic emission event. Compos Sci Technol 2004;64:1819–27. doi:10.1016/j.compscitech.2004.01.008.

[8] Bussiba A, Kupiec M, Ifergane S, Piat R, Böhlke T. Damage evolution and fracture events sequence in various composites by acoustic emission technique. Compos Sci Technol 2008;68:1144–55. doi:https://doi.org/10.1016/j.compscitech.2007.08.032.

[9] Kempf M, Skrabala O, Altstädt V. Reprint of: Acoustic emission analysis for characterisation of damage mechanisms in fibre reinforced thermosetting polyurethane and epoxy. Compos Part B Eng 2014;65:117–23. doi:10.1016/j.compositesb.2014.05.003.

[10] Mohammadi R, Najafabadi MA, Saeedifar M, Yousefi J, Minak G. Correlation of acoustic emission with finite element predicted damages in open-hole tensile laminated composites. Compos Part B Eng 2017;108:427–35. doi:10.1016/j.compositesb.2016.09.101.

[11] Fotouhi M, Saeedifar M, Sadeghi S, Ahmadi Najafabadi M, Minak G. Investigation of the damage mechanisms for mode I delamination growth in foam core sandwich composites using acoustic emission. Struct Heal Monit 2015;14:265–80. doi:10.1177/1475921714568403.

[12] Fotouhi M, Najafabadi MA. Acoustic emission-based study to characterize the initiation of delamination in composite materials. J Thermoplast Compos Mater 2016;29:519–37. doi:10.1177/0892705713519811.

[13] Li L, Lomov S V., Yan X. Correlation of acoustic emission with optically observed damage in

a glass/epoxy woven laminate under tensile loading. Compos Struct 2015;123:45–53. doi:10.1016/j.compstruct.2014.12.029.

[14] Carvelli V, D'Ettorre A, Lomov S V. Acoustic emission and damage mode correlation in textile reinforced PPS composites. Compos Struct 2017;163:399–409. doi:https://doi.org/10.1016/j.compstruct.2016.12.012.

[15] Baker C, Morscher GN, Pujar V V., Lemanski JR. Transverse cracking in carbon fiber reinforced polymer composites: Modal acoustic emission and peak frequency analysis. Compos Sci Technol 2015;116:26–32. doi:10.1016/j.compscitech.2015.05.005.

[16] Maillet E, Baker C, Morscher GN, Pujar V V., Lemanski JR. Feasibility and limitations of damage identification in composite materials using acoustic emission. Compos Part A Appl Sci Manuf 2015;75:77–83. doi:10.1016/j.compositesa.2015.05.003.

[17] ASTM D3039/D3039M-14. Astm D3039/D3039M. Annu B ASTM Stand 2014:1–13. doi:10.1520/D3039.

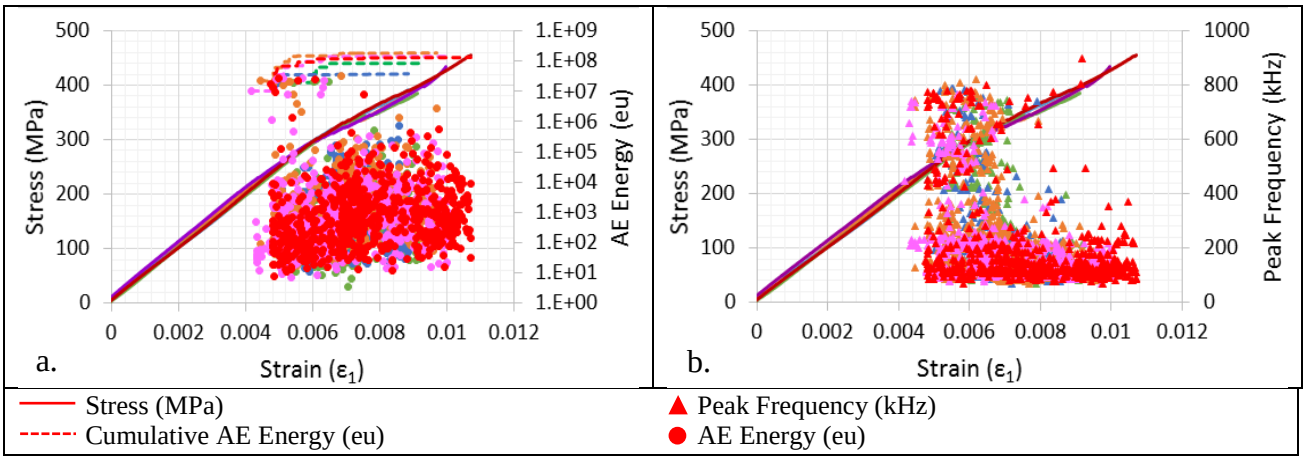

Figure 1. A summary of the stress-strain curves and AE registration for $[-45_2/0_2/+45_2/90_2]_s$ CFRP laminates, data for five specimens are shown with different colours of lines and dots: (a) Stress- and AE energy vs. strain (b) Stress- and peak frequency vs. strain

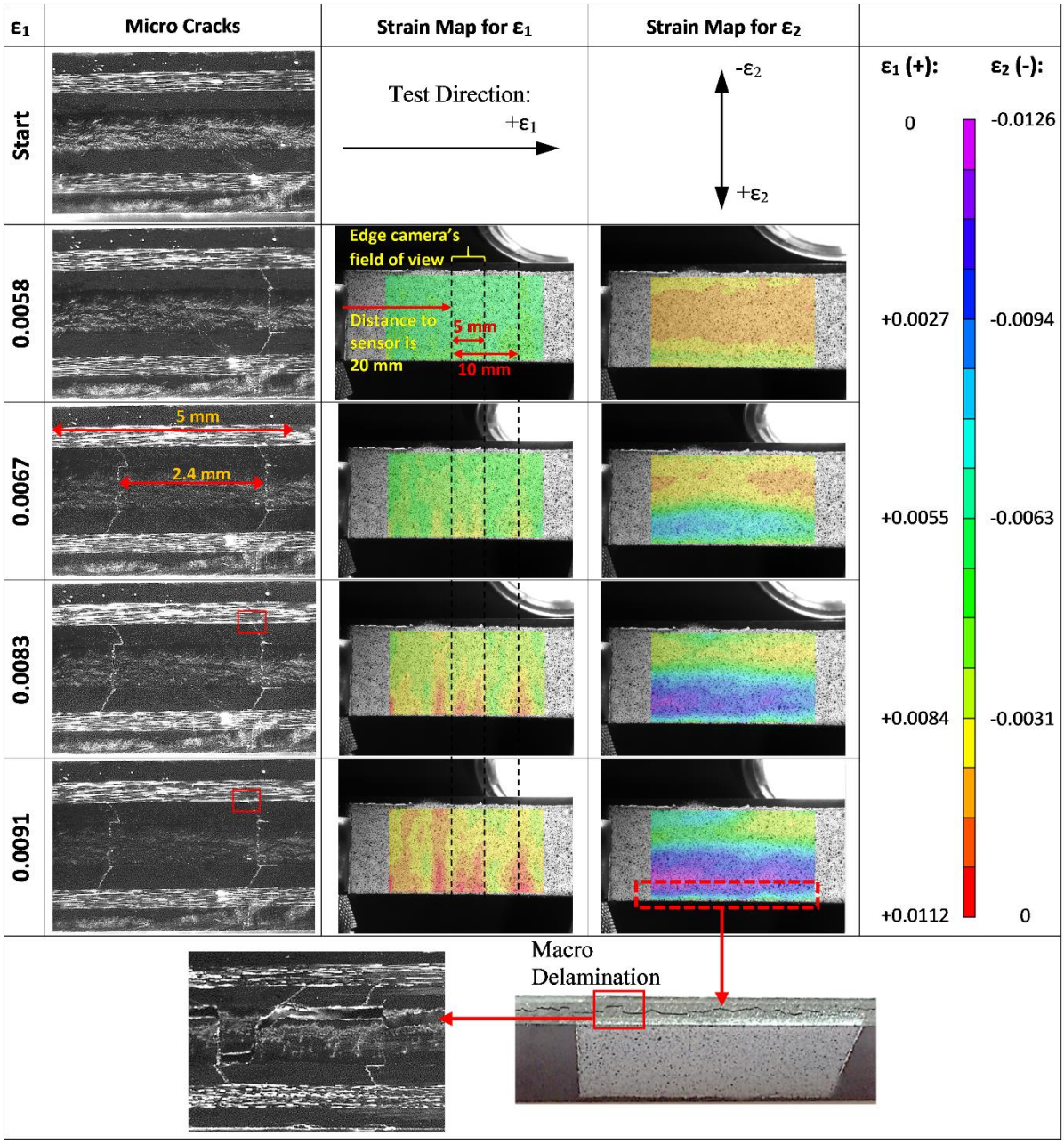

Figure 2. Edge observation and DIC strain map throughout test

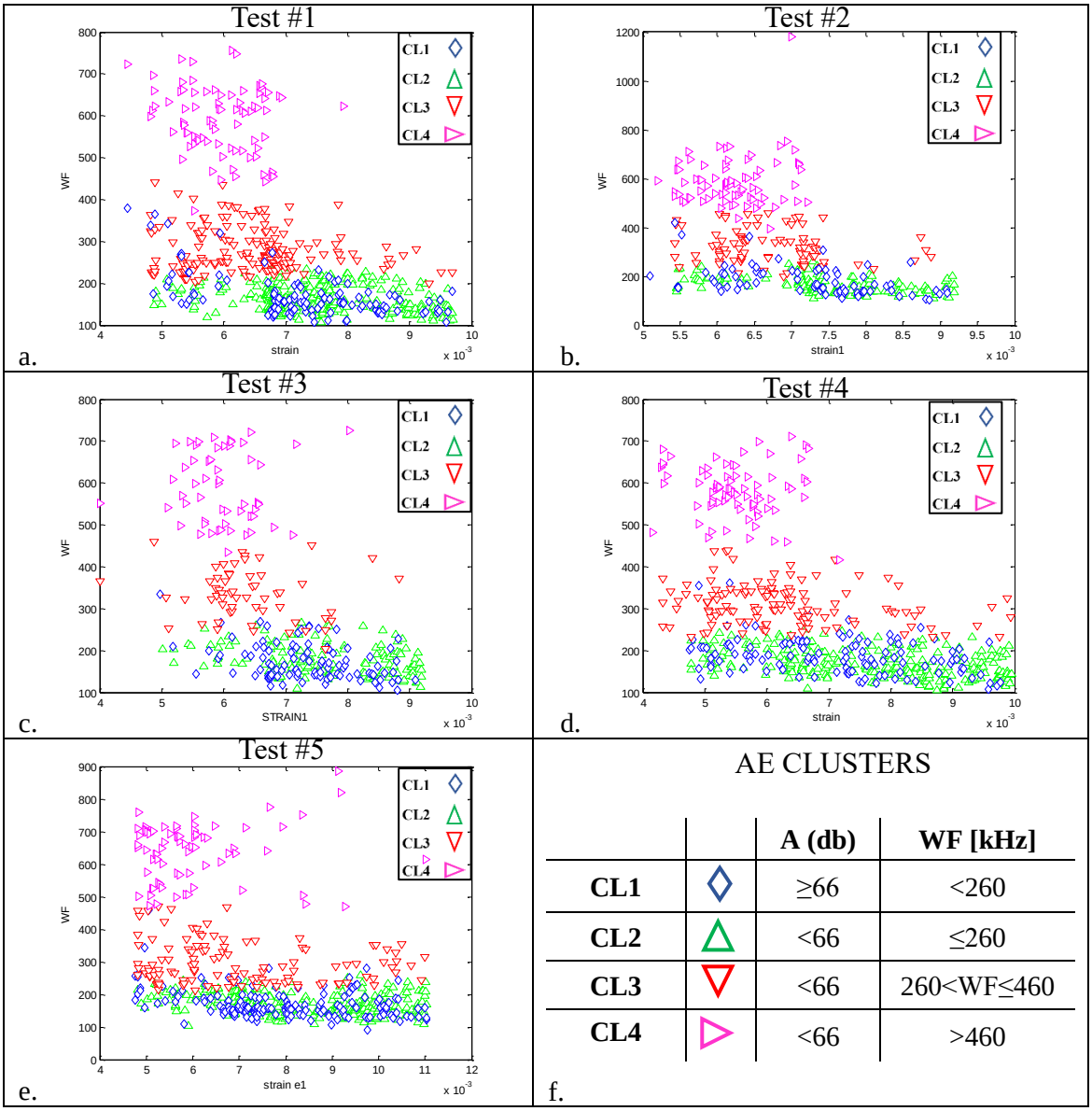

		A (db)	WF [kHz]
CL1	◇	≥66	<260
CL2	△	<66	≤260
CL3	▽	<66	260<WF≤460
CL4	▷	<66	>460

Figure 3. (a-e).Accumulation of AE clusters throughout tests (f) Summary of four clusters.

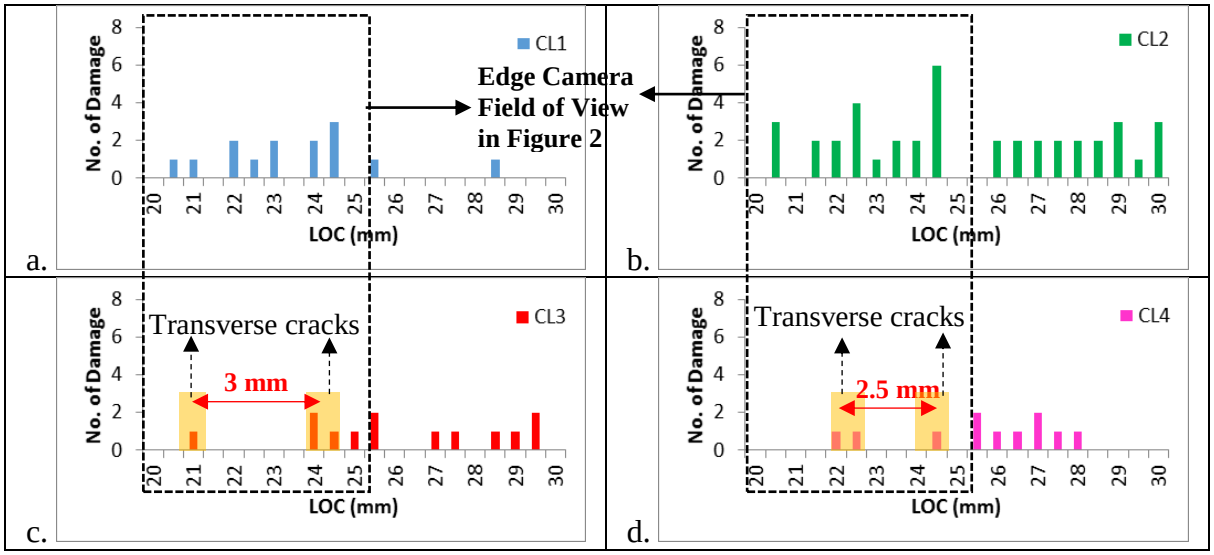

Figure 4. Distribution of AE events in clusters with respect to location during test #3